

New High-Energy Monoenergetic Source for Nanosecond Phonon Spectroscopy*

R. S. Meltzer and J. E. Rives

Department of Physics and Astronomy, University of Georgia, Athens, Georgia 30602

(Received 18 October 1976)

A new monoenergetic nanosecond pulsed source of high-energy phonons is described for doing time-resolved phonon spectroscopy. The phonons, internally generated by excited-state spin-lattice relaxation following optical excitation with a pulsed tunable dye laser, are monitored with nanosecond resolution from enhanced emission of the upper excited state due to resonant absorption. The technique is applied to the determination of the inelastic scattering time of 29-cm^{-1} phonons in ruby ($\tau_p = 530$ ns).

A new technique for performing time-resolved phonon spectroscopy is described which is unique because it utilizes a monoenergetic nanosecond pulsed source of high-energy ($> 10\text{ cm}^{-1}$) phonons. A short burst (3–5 ns) of phonons is produced from spin-lattice relaxation between a pair of excited states after pulsed excitation with a nitrogen-laser-pumped tunable dye laser. The time dependence of the resonant phonon population is monitored optically, with nanosecond time resolution, from the temporal behavior of the emission from the same excited states responsible for the phonon generation.

Although methods are available for the monoenergetic generation of phonons acoustically or with microwaves, they are inherently limited to the low-energy portion of the phonon spectrum. Recently it has been demonstrated that superconducting junctions¹ and infrared radiation sources^{2,3} are capable of generating high-energy monoenergetic phonons. However, these techniques are limited either with respect to type of material and inability to generate the phonons in the bulk, lack of tunability, or maximum energy. None of these sources has been used extensively for studying phonon dynamics.

Several narrow-band optical detectors have been developed for doing phonon spectroscopy in conjunction with either monoenergetic^{2,4} or heat-pulse⁵ sources, but because of limitations on the source or detector, the response time of these systems is > 100 ns. As a result of the increase in phonon scattering rate with frequency,⁶ a faster response will be important in the study of very-high-frequency phonons.

The phonon spectroscopy system we describe has a combination of attributes which make it quite unique: (1) The source serves as its own detector (excited-state resonance) with a ≈ 1 ns response time; (2) the source and detector can simultaneously be tuned, often over a wide range of the phonon spectrum; (3) the phonon source is

highly monoenergetic with a spectral distribution limited by the excited-state resonance width; and (4) the technique is applicable to a wide range of optically transparent materials into which paramagnetic ions can be incorporated.

In order to test this spectroscopy system we have applied it to the direct determination of the inelastic scattering time of 29-cm^{-1} phonons in ruby. Ruby was chosen for this initial test because of the wealth of information available on the dynamics of both its electronically excited states and phonons.

The method is indicated in Fig. 1. A small region of the ruby crystal is excited with a 3-ns pulse from a tunable dye laser tuned to the broad-band absorption at ≈ 5800 Å. These states rapidly relax in a time $T_{\text{band}} \ll 1$ ns, initially producing appreciable populations of $2\bar{A}({}^2E)$ and $\bar{E}({}^2E)$. $2\bar{A}$ then decays to \bar{E} via spin-lattice relaxation in a time $T_1 \approx 0.3$ ns,⁷ releasing into the lattice a monoenergetic⁸ ($\Delta E \approx 0.012\text{ cm}^{-1}$) burst of 29-cm^{-1} phonons. The number of phonons generated ($\approx 10^{13}$) is equal to about half the number of photons absorbed given the $\approx 80\%$ quantum efficiency

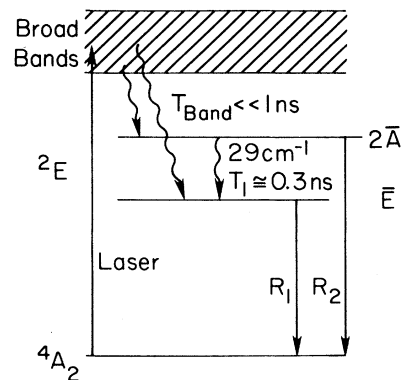


FIG. 1. Description of the phonon source. The broad-band states, after pumping with the tunable dye laser, rapidly decay to $2\bar{A}$ and \bar{E} through single-phonon emission, generating a pulse of 29-cm^{-1} phonons.

for ruby and assuming $2\bar{A}$ and \bar{E} are produced in equal amounts from the broad-band relaxation. The 29-cm^{-1} phonon population is monitored from the enhanced R_2 fluorescence, $2\bar{A}(^2E) \rightarrow ^4A_2$, which results from the absorption of resonant phonons by Cr^{3+} ions in the \bar{E} state, raising the population of $2\bar{A}$ above that characterized by the bath temperature.

The time dependence of the enhanced R_2 fluorescence, obtained using the technique of single-photon time correlation,⁹ immediately after excitation with the laser focused to a spot of radius $r_0 \approx 100 \mu\text{m}$, is shown for a series of pump powers in Fig. 2.

After the initial fast decay, the decay is nearly exponential. At the lowest powers, the enhanced R_2 fluorescence decays with $\tau \approx 15 \text{ ns}$, a time approaching that required for ballistic flight of acoustic phonons across the excited region. At higher pump powers, the phonons become more strongly resonantly scattered due to the higher concentration (N^*) of excited Cr^{3+} , resulting in diffusion-limited (random-walk) migration. The diffusion time τ_d is expected to behave as

$$\tau_d \propto r_0^2/D \propto r_0^2 b(1+b), \quad (1)$$

where D is the diffusion constant and

$$b = N^*/\Sigma = T_1/\tau_{\text{res}}. \quad (2)$$

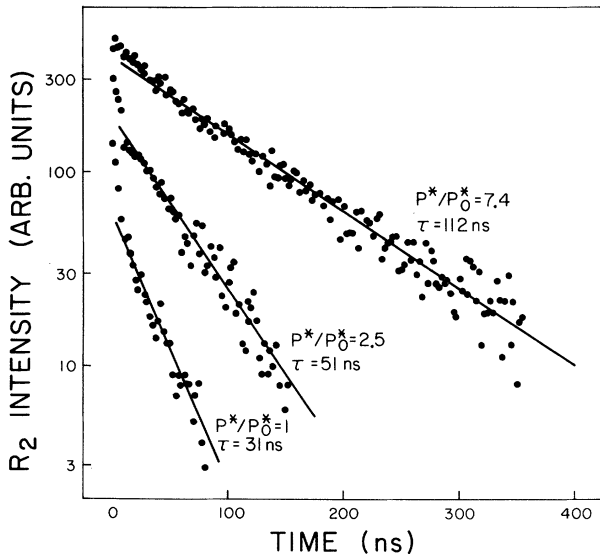


FIG. 2. Decay of the R_2 fluorescence after pumping the broad-band absorption at $\approx 5800 \text{ \AA}$ with the laser focused to a $r_0 \approx 100 \mu\text{m}$ spot on a 2.5-mm-thick ruby sample at 1.5 K. $P^*/P_0^* = 1$ corresponds to the absorption of $\approx 0.5 \mu\text{J}$ of light, producing $\approx 0.8 \times 10^{12}$ phonons in the active volume.

Here $\Sigma = 12\pi\nu^2 d\nu/v^3$ is the number of available re-resonant phonon modes, and τ_{res} is the phonon time of flight between resonant scattering events. The factor $(1+b)^{-1}$ represents the fraction of time the resonant energy exists as a phonon. Under the above conditions, τ is found to be nearly linear in laser power (i.e., N^*) as expected in the region $b < 1$. The rapid decay at short times after the excitation pulse represents emission from the short-lived $2\bar{A}$ state, created from the broad-band relaxation, before it decays to \bar{E} .

To measure τ_p , the inelastic scattering time of these laser-generated 29-cm^{-1} phonons in ruby, one must reduce the other phonon losses so that the inelastic scattering rate becomes a competitive process. This is accomplished by resonantly trapping the phonons in the optically excited region, in a manner similar to that of Renk and Peckenzell.⁵ However, for the maximum values of N^* obtained with $r_0 \approx 100 \mu\text{m}$ in a 2.5-mm-thick 0.06% ruby sample, the decay was diffusion limited with $\tau_d \approx 150 \text{ ns}$.

The diffusive escape time was increased by maintaining these values of N^* over a much larger region of the sample. A 150-W short arc xenon lamp was focused on a $r_0 = 0.5 \text{ mm}$ masked region of the crystal. The lamp was modulated in a pulsed mode of 3-ms duration (45 pps) such that the laser pulse, also illuminating the masked region, occurred at the end of the lamp pulse (maximum N^*). In this way, it was possible to run the lamp well above its rated power so as to maximize N^* . The thickness of the ruby sample was reduced to 1 mm in order to reduce attenuation of the light sources, improving the uniformity of N^* in the optically excited region.

The exponential decay time of R_2 as a function of b (proportional to N^*) is shown in Fig. 3. For small b , the decay time approaches the ballistic propagation time across the 1-mm active region (75–100 ns). As b is increased, the decay time increases due to the diffusive nature of the motion. For large values of b , τ asymptotically approaches a second region linear in b as inelastic scattering dominates the phonon loss.

The observed phonon decay rate is taken as the sum of a diffusive and inelastic rate for the removal of phonons from the excited region.⁵ Thus

$$\tau^{-1} = \tau_d^{-1} + \tau_p^*{}^{-1}, \quad (3)$$

with

$$\tau_d = Ab(1+b) \text{ and } \tau_p^* = \tau_p(1+b), \quad (4)$$

where A is a function of the size and geometry of

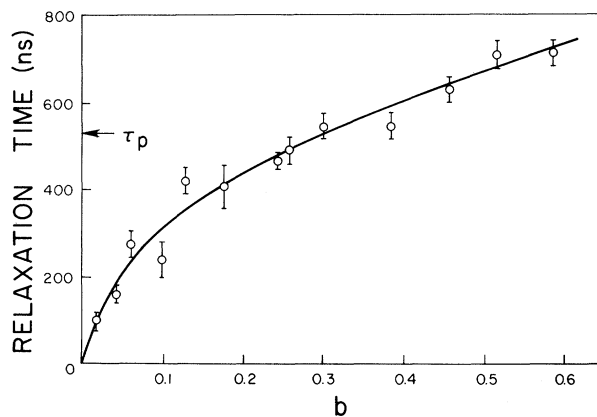


FIG. 3. Dependence of τ , the phonon relaxation time, on b for simultaneous laser and xenon-lamp pumping at 1.5 K. The excitation region was a cylinder 1 mm in the diameter and 1 mm long. The scale on the b axis was obtained from a best fit to the data according to Eqs. (3) and (4), shown by the solid curve, with $\tau_p = 530$ ns and $A = 11\tau_p$.

the excitation region, ν , and T_1 .¹⁰ This description provides a good fit to the data, as shown by the solid curve in Fig. 3, with $\tau_p = 530 \pm 150$ ns. With the highest values of N^* available in these measurements [$\approx 2 \times 10^{16}/\text{cm}^3$, estimated from Eq. (2)], the phonon decay rate is dominated by the inelastic scattering, although the diffusive migration out of the excited region still plays a significant role ($\tau_p^* = 850$ ns, $\tau_d = 5700$ ns). Although the value of τ_p is about a third that originally observed by Renk and Peckenzell,⁵ it is in very good agreement with Renk's more recent measurements.¹¹

If we assume that phonons are generated in both the transverse and the longitudinal modes, the small value of τ_p suggests that there is significant mode conversion between the long-lived transverse and shorter-lived longitudinal modes,¹² presumably by resonant scattering. The above measured value of τ_p therefore represents some average over the modes, with τ_p for the longitudinal modes somewhat smaller since only a fraction of the phonons occupy these modes.

The nearly exponential decay of R_2 in all of these measurements suggests that little or no spectral diffusion occurs during the phonon decay time. Spectral diffusion would produce a time-dependent reduction in b through an increase in Σ , resulting in an increase in the relaxation rate as the decay proceeds. This conclusion is consistent with the results of Dijkhuis, van der Pol, and de Wijn¹³ who found that even at their lowest N^* ($\approx 10^{17}/\text{cm}^3$), little spectral redistribution oc-

curred.

We emphasize that there is no upper limit on the energy of the phonons which can be studied except that the spin-lattice relaxation must be faster than the time domain of the dynamical processes of interest and the enhanced emission due to the presence of resonant phonons must be sufficient for detection. It should be possible to meet these conditions for a large number of systems at even higher resonant phonon energies than in ruby. Systems containing rare-earth ions will be of special interest since in many cases the resonant phonon energy can be tuned with a magnetic field and with the selection of several spin-lattice coupled crystal-field states with different energy gaps, making it possible to perform high-resolution phonon spectroscopy in both the energy and temporal domains. These techniques should therefore prove highly useful for identifying the mechanisms and testing the theoretical models for the scattering of high-energy phonons.

We remark finally that in most systems tunable-dye-laser excitation is capable of generating a total spin inversion within the excited states,¹⁴ making it possible to study the recently suggested possibility of spin-phonon superradiance in paramagnetic systems,¹⁵ as well as phonon amplification which has been observed previously in the ground state.¹⁶

We thank Dr. William Yen for lending us the ruby samples.

*Research sponsored in part by National Science Foundation Grants No. DMR 76-10855, No. DMR 73-02606 A01, and No. DMR 71-01779 A02.

¹R. C. Dynes and V. Narayanamurti, Phys. Rev. B **6**, 143 (1972).

²M. J. Colles and J. A. Giordmaine, Phys. Rev. Lett. **27**, 670 (1971).

³W. Grill and O. Weis, Phys. Rev. Lett. **35**, 588 (1975).

⁴C. H. Anderson and E. S. Sabisky, in *Physical Acoustics*, edited by W. P. Mason and R. Thurston (Academic, New York, 1971), Vol. 8.

⁵K. F. Renk and J. Peckenzell, J. Phys. (Paris), Colloq. **33**, C4-103 (1972).

⁶P. Carruthers, Rev. Mod. Phys. **33**, 92 (1961).

⁷M. Blume, R. Orbach, A. Kiel, and S. Geschwind, Phys. Rev. **139**, A314 (1965).

⁸H. Lengfellner, G. Pauli, W. Heisel, and K. F. Renk, Appl. Phys. Lett. **29**, 566 (1976).

⁹R. S. Meltzer and R. M. Wood, to be published.

¹⁰A rigorous treatment of the diffusion would have to take account of the anisotropy and branch dependence of the spin-lattice coupling as well as the actual distribution of phonons among the three branches. Since

little is known about these effects, A is taken to be some average which is to be determined empirically.

¹¹K. F. Renk, private communication.

¹²For transverse phonons $\tau_p \approx 10^{-2}$ sec. See, e.g., R. Orbach and L. A. Vredevoe, *Physics* **1**, 91 (1964).

¹³J. I. Dijkhuis, A. van der Pol, and H. W. de Wijn, *Phys. Rev. Lett.* **37**, 1554 (1976).

¹⁴R. S. Meltzer and J. E. Rives, *Phys. Rev. B* (to be published).

¹⁵C. Leonardi, J. C. MacGillivray, S. Liberman, and M. S. Feld, *Phys. Rev. B* **11**, 3298 (1975).

¹⁶E. B. Tucker, *Phys. Rev. Lett.* **6**, 547 (1961); E. M. Ganapol'skii and D. N. Makovetskii, *Solid State Commun.* **15**, 1249 (1974).

Energy Dependence of Defect Production in Displacement Cascades in Silver*

K. L. Merkle, R. S. Averback, and R. Benedek

Materials Science Division, Argonne National Laboratory, Argonne, Illinois 60439

(Received 29 November 1976)

Proton damage rates in Ag measured below 10 K show good agreement with calculated defect-production cross sections for low-energy recoils. A substantial decrease in damage efficiency (from $\bar{\xi} = 1$ to $\bar{\xi} \approx 0.6$) occurs as the energy and/or mass of the incident particle increases and displacement cascades are produced. Preliminary results are consistent with cascade efficiencies near $\xi = 0.3$ and an effective transition from $\xi = 1$ to $\xi = 0.3$ centered near recoil energies between 1 and 3 keV.

The determination of displacement damage-production rates in radiation environments, especially for fission and fusion reactors, is of considerable technological interest. For the past twenty years, a serious discrepancy has existed between the theoretical and experimental estimates of Frenkel-pair production in energetic displacement cascades in pure metals. Notably, it was found that, for fast neutron and ion bombardment, the experimental damage rates were a factor of 2 to 3 lower than predicted by theory.^{1,2}

In this Letter, we report some preliminary results on the energy dependence of light-ion damage in Ag, as determined by residual-resistivity measurements on thin-film specimens. The defect production rates show good agreement with theory when predominantly isolated Frenkel pairs (FP) are produced. However, as the energy and/or mass of the incident ion increases, a substantial decrease in damage efficiency is observed when recoils near and above 2 keV contribute significantly to the damage production. The decrease in damage-production efficiency is considerably stronger than can be accounted for by the modified Kinchin-Pease formulation and computer simulations of cascades that use the binary-collision approach.^{3,4}

Thin Ag films with a thickness of 0.2–0.5 μm were grown by vapor deposition onto rock salt. The films were transferred to irradiation holders and irradiated below 10 K with several light ions ranging in mass from 1–20 amu. In each instance, the projected range was substantially greater than the film thickness. The number of

defects produced was determined by measuring the resistivity changes $\Delta\rho$. Care was taken to minimize radiation annealing effects by taking measurements predominantly at low defect concentrations ($\Delta\rho < 2 \times 10^{-8} \Omega \text{ cm}$). By utilizing the nearly linear decrease in damage rate as a function of induced resistivity for Ag irradiated with protons at a fixed energy, the measured damage rates were corrected for both radiation annealing and electrical size effect. For the size-effect correction, the Fuchs-Sondheimer theory was used in combination with an accurate determination of the size-effect parameters from proton-damage curves. Multiple scattering of the beam increases the path length in the film and therefore the damage produced. A correction for this effect was included and was < 1% for ions lighter than boron, as estimated from calculations of the half-width of angular distributions.⁵ The initial damage rates $(d\Delta\rho/d\phi)_0$ obtained in this manner were used to determine the number of FP's produced per atom and incident ion, i.e., the FP production cross section $\sigma_F(\bar{E}) = (d\Delta\rho/d\phi)_0 \rho_F^{-1}$. Here ρ_F is the FP resistivity. The average energy of the beam in the foil is a good approximation of the energy \bar{E} associated with this cross section.⁶ \bar{E} was determined from the incident energy E_0 , electronic⁷ and nuclear⁸ stopping-power data, and the gravimetrically determined film thickness. The cross sections for protons on silver are given in Fig. 1, which also includes the data of Andersen and Sørensen.⁹

In the past, a comparison of damage-rate data with cascade theory has been difficult because